Indian Journal of Pure & Applied Physics
Vol. 56, February 2018, pp. 119-127

Vibrational analysis, *ab initio* HF and DFT studies of 2,4,6-trimethyl phenol

S Prabhakaran & M Jamal Mohamed Jaffar*

PG & Research Department of Physics, Jamal Mohamed College,
Tiruchirappalli 620 020, India

Received 2 November 2016; accepted 2 November 2017

The Fourier transform infrared (FTIR) and FT-Raman spectra of 2,4,6-trimethylphenol have been recorded in the range 4000–400 and 3500–100 cm^{-1}, respectively. The complete vibrational assignment and analysis of the fundamental modes of the compound have been carried out using the observed FTIR and FT-Raman data. The vibrational frequencies determined experimentally have been compared with those obtained theoretically from *ab initio* HF and DFT-B3LYP gradient calculations employing 6-31+G (d,p) basis sets for the optimized geometries of the compound. The geometries and normal modes of vibration obtained from the HF and DFT methods are in good agreement with the experimental data. The normal coordinate analysis has also been carried out with *ab initio* force fields utilizing Wilson's FG matrix method. The interactions of the skeletal vibrational modes have been investigated.

Keywords: FTIR, FT-Raman, DFT calculations, Vibrational assignment, TMP

1 Introduction

Phenol, also known as carbolic acid, is an organic compound. It is produced on a large scale as a precursor to many materials and useful compound. Phenol is also a versatile precursor to a large collection of drugs, most notably aspirin but also many herbicides and pharmaceuticals. It is used in the preparation of cosmetics including sunscreens, hair dyes and skin lightening preparations. Phenol and its vapors are corrosive to the eyes, the skin and the respiratory tract. The major uses of phenol involve its conversion to plastics or related materials. Phenol derivatives are interesting molecules for theoretical studies due to their relatively smaller size and similarity to biological species. The vibrational spectrum of phenol was extensively studied and analyzed[1-3]. Literature survey

[illegible] Therefore, we have undertaken the detailed theoretical and experimental investigation of the vibrational spectra of the molecule. Density Functional B3LYP calculations have been performed to support our assignments.

Density functional theory calculations[4] are also reported to provide excellent vibrational frequencies of organic compounds, if the calculated frequencies are scaled to compensate for the approximate treatment of electron correction, for basis set deficiencies and for the anharmonicity effects[5-9]. Electronic structure methods, namely, *ab initio* HF self- consistent field method and density functional methods are increasingly used by spectroscopists for modeling molecular properties that include equilibrium structure vibrational frequencies and intensities[10].

To the best of our knowledge, no theoretical HF or DFT calculations or detailed vibrational infrared and Raman analysis have been performed on TMP molecule. A detailed quantum chemical study will aid in understanding the vibrational modes of this title compounds. So, in this present work, the vibrational wave numbers, geometrical parameters, modes of vibrations, dipole moment, reduced mass, force constant and other thermodynamic parameters of TMP [illegible] and B3LYP calculations with 6-31+G(d,p) basis set. Specific scale factors were also used and employed in the predicted frequencies.

2 Experimental Methods

The compound TMP obtained from Lancaster chemical company, UK and used as such without any further purification. The FT-Raman spectra of TMP have been recorded using a 1064 nm line of Nd:YAG laser as excitation wavelength in the region 3500-50 cm^{-1} on a BRUKER IFS 66V spectrophotometer equipped with FRA 106 FT-Raman module accessory. The FTIR spectrum of this compound was

*Corresponding author (E-mail: jmjaffar@yahoo.com)

recorded in the region 4000 - 400 cm^{-1} on BRUKER IFS 66V spectrophotometer using KBr pellet technique.

The entire calculations were performed at HF and B3LYP levels using GAUSSIAN 09 Windows[11] program package involving gradient geometry optimization[12]. Initial geometry generated from standard geometrical parameters was minimized without any constraint in the potential energy surface at HF and B3LYP levels adopting the standard 6-31+G (d,p) basis set. This geometry was then re-optimized again at the B3LYP level, using basis set 6-31+G(d,p). The optimized structural parameters were used in the vibrational frequency calculations at the DFT levels to characterize all stationary points as minima. We have utilized the gradient corrected density functional theory[13] (DFT) with the three parameters hybrid functional[14] (B3) for the exchange part and Lee-Yang-Parr (LYP) correlation function[15], accepted as a cost-effective approach, for the computation of molecular structure, vibrational frequencies and energies of optimized structures. Vibrational frequencies computed at DFT level have been adjudicated to be more reliable than those obtained by the computationally demanding Moller-Plesset perturbation methods. Density functional theory offers electron correlation frequently comparable to second-order Moller-Plesset theory (MP2). Finally, the calculated normal mode vibrational frequencies provide thermodynamic properties also through the principle of statistical mechanics.

By combining the results of the GAUSSVIEW program[16] with symmetry considerations vibrational frequency assignments were made with a high degree of accuracy. There is always some ambiguity in defining internal coordination. However, the defined coordinate forms complete set and matches quite well with the motions observed using the GAUSSVIEW program. Raman intensities (I_i) using the following relationship derived from basic theory of Raman scattering[17,18].

$$I_i = \frac{f(\nu_0 - \nu_1)^4 S_i}{\nu_i \left[1 - exp\left(\frac{hc\nu_i}{kT}\right)\right]}$$

where ν_o is the exciting frequency (in cm^{-1} units), ν_i is the vibrational wavenumber for the i^{th} normal modes, h, c and k are fundamental constants and f is a suitable chosen common normalization factor for all peak intensities.

3 Results and Discussion

3.1 Molecular geometry

The optimized molecular structure of TMP having C_1 symmetry is shown in Fig. 1. The global minimum energy obtained by the HF and DFT structure optimization for TMP, were calculated as –422.70193282 and –425.45596685 Hartrees, from 6-31+G (d,p) basis set, respectively. The optimized geometrical parameters obtained by the large basis set calculations for TMP are presented in Table 1.

A detailed description of vibrational modes is given by means of normal coordinate analysis (NCA). For this purpose, the full set of 75 standard internal coordinates (containing 15 redundancies) for the title compound is presented in Table 2. From these, a non-redundant set of local symmetry coordinates are constructed by suitable linear combinations of internal coordinates following the recommendations of Pulay and Fogarasi which are summarized in Table 3. The theoretically calculated DFT force fields were transformed to this set of vibrational coordinates and used in all subsequent calculations.

3.2 Vibrational Spectra

The optimized structural parameters were used to compute the vibrational frequencies of TMP at the HF and B3LYP level with 6-31+G(d,p) basis set. From the structural point of view, the molecule is assumed to have C_1 point group symmetry and hence, all the calculated frequency transforming to the same symmetry species (A). The molecule TMP consists of 22 atoms and expected to have 60 normal modes of

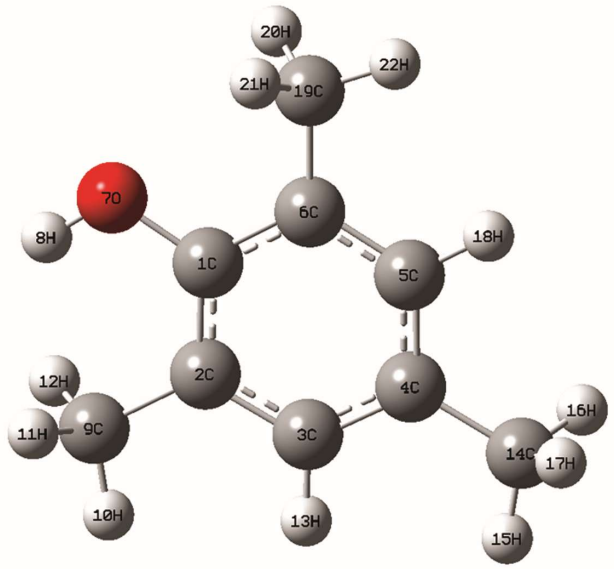

Fig. 1 — Molecular structure of 2,4,6-trimethylphenol.

Table 1 — Optimized geometrical parameters of 2,4,6-trimethylphenol obtained by HF and B3LYP using 6-31+G(d,p) basis set calculations.

Parameter bond length	Value (Å)		Bond angle	Value (°)		Dihedral Angle	Value (°)	
	HF	B3LYP		HF	B3LYP		HF	B3LYP
C1-C2	1.3869	1.4026	C2-C1-C6	121.5268	121.6991	C6-C1-C2-C3	0.0009	0.1062
C1-C6	1.3955	1.4051	C2-C1-O7	122.1702	122.0006	C6-C1-C2-C9	180.0016	-179.7411
C1-O7	1.3609	1.3789	C6-C1-O7	116.303	116.3	O7-C1-C2-C3	-180.0029	179.8806
C2-C3	1.3947	1.402	C1-C2-C3	118.2457	118.0958	O7-C1-C2-C9	-0.0021	0.0333
C2-C9	1.5123	1.5117	C1-C2-C9	120.9394	120.7048	C2-C1-C6-C5	-0.0014	-0.1187
C3-C4	1.3834	1.3975	C3-C2-C9	120.8148	121.1992	C2-C1-C6-C19	-180.0022	179.7318
C3-H13	1.077	1.0881	C2-C3-C4	122.0622	122.1348	O7-C1-C6-C5	180.0021	-179.9053
C4-C5	1.3938	1.4024	C2-C3-H13	118.5066	118.4884	O7-C1-C6-C19	0.0013	-0.0547
C4-C14	1.5119	1.5124	C4-C3-H13	119.4312	119.3767	C2-C1-O7-H8	-0.0216	0.13
C5-C6	1.3839	1.3971	C3-C4-C5	117.7929	117.7787	C6-C1-O7-H8	-180.0251	179.9159
C5-H18	1.0776	1.0884	C3-C4-C14	121.6025	121.3149	C1-C2-C3-C4	-0.0003	0.07
C6-C19	1.5088	1.5081	C5-C4-C14	120.6045	120.9003	C1-C2-C3-H13	-179.9991	-179.8671
O7-H8	0.9414	0.9651	C4-C5-C6	122.2087	122.3329	C9-C2-C3-C4	-180.0011	179.9165
C9-H10	1.0827	1.0929	C4-C5-H18	119.1943	119.2766	C9-C2-C3-H13	0.0002	-0.0206
Parameter bond length	Value (Å)		Bond angle	Value (°)		Dihedral Angle	Value (°)	
	HF	B3LYP		HF	B3LYP		HF	B3LYP
C9-H11	1.0883	1.0991	C6-C5-H18	118.597	118.3904	C1-C2-C9-H10	-180.0059	179.9556
C9-H12	1.0883	1.0991	C1-C6-C5	118.1636	117.9582	C1-C2-C9-H11	-60.6126	-60.6986
C14-H15	1.0842	1.0943	C1-C6-C19	119.942	120.038	C1-C2-C9-H12	60.6022	60.5844
C14-H16	1.0862	1.0957	C5-C6-C19	121.8944	122.0036	C3-C2-C9-H10	-0.0052	0.1131
C14-H17	1.0862	1.0974	C1-O7-H8	111.9087	110.1003	C3-C2-C9-H11	119.3882	119.4588
C19-H20	1.0851	1.0959	C2-C9-H10	110.6111	110.6784	C3-C2-C9-H12	-119.397	-119.2581
C19-H21	1.0851	1.0935	C2-C9-H11	111.8566	112.1986	C2-C3-C4-C5	0.0003	-0.2227
C19-H22	1.0838	1.0959	C2-C9-H12	111.8562	112.2138	C2-C3-C4-C14	179.9884	178.8852
			H10-C9-H11	107.1763	106.9241	H13-C3-C4-C5	179.9991	179.7138
			H10-C9-H12	107.1753	106.9363	H13-C3-C4-C14	-0.0128	-1.1783
			H11-C9-H12	107.9284	107.5931	C3-C4-C5-C6	-0.0009	0.2096
			C4-C14-H15	111.1311	111.3101	C3-C4-C5-H18	-179.9977	-179.7047
			C4-C14-H16	111.2298	111.502	C14-C4-C5-C6	-179.9891	-178.9021
			C4-C14-H17	111.2271	111.4485	C14-C4-C5-H18	0.014	1.1835
			H15-C14-H16	107.7668	107.7644	C3-C4-C14-H15	0.077	14.9116
			H15-C14-H17	107.7653	107.4376	C3-C4-C14-H16	120.1498	135.2873
Parameter bond length	Value (Å)		Bond angle	Value (°)		Dihedral Angle	Value (°)	
	HF	B3LYP		HF	B3LYP		HF	B3LYP
			H16-C14-H17	107.5462	107.1594	C3-C4-C14-H17	-119.992	-105.0122
			C6-C19-H20	111.0719	111.3007	C5-C4-C14-H15	-179.9352	-166.0083
			C6-C19-H21	111.0707	110.7735	C5-C4-C14-H16	-59.8624	-45.6325
			C6-C19-H22	110.5733	111.3073	C5-C4-C14-H17	59.9958	74.0679
			H20-C19-H21	107.0805	108.3905	C4-C5-C6-C1	0.0014	-0.0439
			H20-C19-H22	108.4613	106.5111	C4-C5-C6-C19	180.0023	-179.8913
			H21-C19-H22	108.4589	108.3954	H18-C5-C6-C1	179.9983	179.8712
						H18-C5-C6-C19	-0.0009	0.0238
						C1-C6-C19-H20	-59.5179	59.3912
						C1-C6-C19-H21	59.5449	-179.9402
						C1-C6-C19-H22	-179.9884	-59.261
						C5-C6-C19-H20	120.4813	-120.7645
						C5-C6-C19-H21	-120.456	-0.0959
						C5-C6-C19-H22	0.0107	120.5833

vibrations. All the vibrations are active both in the Raman scattering and infrared absorption.

The observed and calculated frequencies and the detailed vibrational assignment of fundamental modes of TMP along with the calculated IR and Raman intensities, reduced mass, force constants and normal mode description (characterized) by TED are reported in Table 4. The FTIR and FT-Raman spectra of TMP are shown in Figs 2 and 3, respectively.

Table 2 — Definition of internal coordinates of 2,4,6-trimethylphenol.

No	Symbol	Type	Definition[a]
Stretching			
1 – 2	r_i	C-H	C3-H13, C5-H18
3 – 11	r_i	C-H (Methyl)	C9-H10, C9-H11, C9-H12, C14-H15, C14-H16, C14-H17, C19-H20, C19-H21, C19-H22
12	Q_i	C-O	C1-O7
13	S_i	O-H	O7-H8
14 – 22	R_I	C-C	C1-C2, C2-C3, C3-C4, C4-C5, C5-C6, C6-C1, C2-C9, C4-C14, C6-C19
In-plane bending			
23 – 28	β_i	Ring	C1-C2-C3, C2-C3-C4, C3-C4-C5, C4-C5-C6, C5-C6-C1, C6-C1,C2
29 – 32	α_i	C-C-H	C2-C3-H13, C4-C3-H13, C4-C5-H18, C6-C5-H18
33 – 41	α_I	C-C-H (Methyl)	C2-C9-H10, C2-C9-H11, C2-C9-H12, C4-C14-H15, C4-C14-H16, C4-C14-H17, C6-C19-H20, C6-C19-H21, C6-C19-H22
42 – 43	γ_i	C-C-O	C2-C1-O7, C6-C1-O7
44 – 49	δ_i	C-C-C	C1-C2-C9, C3-C2-C9, C3-C4-C14, C5-C4-C14, C5-C6-C19, C1-C6-C19
50	ξ_i	C-O-H	C1-O7-H8
51 – 59	σ_i	H-C-H	H10-C9-H11, H11-C9-H12, H10-C9-H12, H15-C14-H16, H16-C14-H17, H15-C14-H17, H20-C19-H21, H21-C19-H22, H20-C19-H22
No	Symbol	Type	Definition[a]
Out-of-plane bending			
60 – 61	ω_i	C-H	H13-C3-C2-C4, H18-C5-C4-C6
62	π_i	O-C	O7-C1-C2-C6
63	ρ_i	O-H	H8-O7-C1-(C2, C6)
64 – 66	γ_i	C-C	C9-C2-C1-C3, C14-C4-C3-C5, C19-C6-C1-C5
Torsion			
67 – 72	t_i	t Ring	C1-C2-C3-C4, C2-C3-C4-C5, C3-C4-C5-C6, C4-C5-C6-C1, C5-C6-C1-C2, C6-C1-C2-C3
73 – 75	t_I	t C-CH_3	(C1, C3) - C2 - C9 - (H10, H11, H12) (C3, C5) - C4 - C14 - (H15, H16, H17) (C1, C5) - C6 - C19 - (H20, H21, H22)

Table 3 — Definition of local symmetry coordinates of 2,4,6-trimethylphenol.

No	Symbol[a]	Definition[b]
1 – 2	CH	r_1, r_2
3 – 5	CH_3 ss	$(r_3 + r_4 + r_5)/\sqrt{3}$, $(r_6 + r_7 + r_8)/\sqrt{3}$, $(r_9 + r_{10} + r_{11})/\sqrt{3}$
6 – 8	CH_3 ips	$(2r_3 + r_4 + r_5)/\sqrt{6}$, $(2r_6 + r_7 + r_8)/\sqrt{6}$, $(2r_9 + r_{10} + r_{11})/\sqrt{6}$
9 – 11	CH_3 ops	$(r_4 - r_5)/\sqrt{2}$, $(r_7 - r_8)/\sqrt{2}$, $(r_{10} - r_{11})/\sqrt{2}$
12	CO	Q_{12}
13	OH	S_{13}
14 – 22	CC	R_{14}, R_{15}, R_{16}, R_{17}, R_{18}, R_{19}, R_{20}, R_{21},R_{22}
23	R trigd	$(\beta_{23} - \beta_{24} + \beta_{25} - \beta_{26} + \beta_{27} - \beta_{28})/\sqrt{6}$
24	R symd	$(-\beta_{23} - \beta_{24} + 2\beta_{25} - \beta_{26} - \beta_{27} + 2\beta_{28})/\sqrt{12}$
25	R asymd	$(\beta_{23} - \beta_{24} + \beta_{26} - \beta_{27})/2$
26 – 27	b CH	$(\alpha_{29} - \alpha_{30})/\sqrt{2}$, $(\alpha_{31} - \alpha_{32})/\sqrt{2}$
28 – 30	CH_3 sb	$(\alpha_{33} - \alpha_{34} - \alpha_{35} + \sigma_{36} + \sigma_{37} + \sigma_{38})/\sqrt{6}$, $(\alpha_{39} - \alpha_{40} - \alpha_{41} + \sigma_{42} + \sigma_{43} + \sigma_{44})/\sqrt{6}$, $(\alpha_{45} - \alpha_{46} - \alpha_{47} + \sigma_{48} + \sigma_{49} + \sigma_{50})/\sqrt{6}$,
31 – 33	CH_3 ipb	$(-\sigma_{68} - \sigma_{39} - 2\sigma_{40})/\sqrt{6}$, $(-\sigma_{44} - \sigma_{45} - 2\sigma_{46})/\sqrt{6}$, $(-\sigma_{48} - \sigma_{49} - 2\sigma_{50})/\sqrt{6}$,
34 – 36	CH_3 opb	$(\sigma_{38} - \sigma_{39})/\sqrt{2}$, $(\sigma_{44} - \sigma_{45})/\sqrt{2}$, $(\sigma_{48} - \sigma_{49})/\sqrt{2}$,
37 – 39	CH_3 ipr	$(2\alpha_{35} - \alpha_{36} - \alpha_{37})/\sqrt{6}$, $(2\alpha_{41} - \alpha_{42} - \alpha_{43})/\sqrt{6}$, $(2\alpha_{47} - \alpha_{48} - \alpha_{49})/\sqrt{6}$,
40 – 42	CH_3 opr	$(\alpha_{36} - \alpha_{37})/\sqrt{2}$, $(\alpha_{42} - \alpha_{43})/\sqrt{2}$, $(\alpha_{48} - \alpha_{49})/\sqrt{2}$,
43	b CO	$(\gamma_{51} - \gamma_{52})/\sqrt{2}$,
44 – 46	b CC	$(\delta_{53} - \delta_{54})/\sqrt{2}$, $(\delta_{55} - \delta_{56})/\sqrt{2}$, $(\delta_{57} - \delta_{55})/\sqrt{2}$,
No	Symbol[a]	Definition[b]
47	b OH	ξ_{59}
48 – 49	ω CH	ω_{60}, ω_{61}
50	ω OC	π_{62}
51	ω OH	ρ_{63}
52 – 54	ω CC	γ_{64}, γ_{65}, γ_{66}
55	t Rtrig	$\tau_{67} - \tau_{68} + \tau_{69} - \tau_{70} + \tau_{71} - \tau_{72})/\sqrt{6}$
56	t Rsym	$(\tau_{67} - \tau_{69} + \tau_{70} - \tau_{72})/\sqrt{2}$
57	t Rsym	$(-\tau_{67} + 2\tau_{68} - \tau_{69} - \tau_{70} + 2\tau_{71} - \tau_{72})/\sqrt{12}$
58 – 60	t CH_3	τ_{73}, τ_{74}, τ_{75}

3.2.1 O–H group vibrations

Hydrogen bonding alters the frequencies of the stretching and bending vibration. The O-H stretching bands move to lower frequencies usually with increased intensity and band broadening in the hydrogen bonded species. Hydrogen bonding if present in five or six member ring system would reduce the O-H stretching band to 3200-3550 cm^{-1} region[19]. The O-H in-plane-bending vibration in phenol, in general, lies in the region 1150-1250 cm^{-1} and is not much affected due to hydrogen bonding unlike the stretching and out-of-plane deformation frequencies. The O-H out-of-plane

Table 4 — The observed FTIR, FT-Raman and calculated (unscaled and scaled) frequencies (cm^{-1}), IR intensity (km mol^{-1}), Raman Activity ($Å^4$ amu^{-1}), and probable assignments (characterized by TED) of 2,4,6-trimethylphenol using HF/6-31+G(d,p) and B3LYP/6-31+G(d,p) calculations.

Species	Observed wave numbers (cm^{-1})										
	FTIR	FT Raman	Unscaled	Scaled	IR intensity	Raman active	Unscaled	Scaled	IR intensity	Raman active	Assignments
A	3396 (s)	-	4219	3412	94.5646	60.9359	3843	3402	59.1577	82.4816	νOH (99)
A	-	3380 (w)	3335	3398	19.7147	98.0702	3165	3386	11.4069	141.4477	νCH (98)
A	-	3100 (s)	3329	3112	25.3010	80.0126	3163	3105	29.5056	64.2694	νCH (96)
A	-	3019 (w)	3269	3025	18.3736	56.5309	3122	3024	13.7496	61.2399	CH_3ss (92)
A	3013 (w)	-	3264	3019	26.0454	63.5454	3121	3019	16.3158	62.8403	CH_3ss (94)
A	-	2980 (w)	3255	2988	26.3565	62.4871	3111	2988	18.3483	63.7400	CH_3ss (91)
A	2973(ms)	-	3247	2983	23.4498	82.4407	3091	2970	15.9941	91.8800	CH_3ips (90)
A	2944 (w)	-	3230	2951	28.4780	83.9146	3083	2949	20.6421	94.3425	CH_3ips (89)
A	2917 (w)	2918 (w)	3206	2925	30.9746	85.3562	3053	2915	22.1331	96.6577	CH_3ips (88)
A	2857(ms)	-	3189	2865	41.4264	191.3184	3038	2853	34.2210	248.1896	CH_3 ops (90)
A	-	2850 (w)	3178	2860	51.1588	178.9046	3029	2847	47.7913	243.7076	CH_3ops (91)
A	-	2740 (w)	3161	2748	49.0219	170.9271	3008	2739	44.1165	223.9733	CH_3 ops (87)
A	1740 (s)	-	1807	1747	0.0079	15.4485	1658	1742	0.1009	20.9929	νCC (86)
A	1728(vw)	-	1800	1735	5.9648	15.5750	1650	1730	3.5568	18.7926	νCC (87)
A	-	1720 (w)	1657	1729	103.7226	4.5233	1530	1722	83.3311	3.9679	νCC (85)
A	-	1640 (vw)	1632	1648	19.9148	9.1012	1513	1638	23.1319	8.3127	νCC (84)
A	1612 (s)	-	1620	1620	5.9386	0.7822	1500	1610	2.3411	1.5284	νCC (82)
A	-	1604 (vw)	1614	1614	6.8782	11.9531	1496	1600	7.887	10.6158	νCC (83)
A	-	1495 (w)	1608	1492	4.2031	10.7561	1491	1491	5.2912	9.8333	νCC (85)
Species	Observed wave numbers (cm^{-1})										
	FTIR	FT Raman	Unscaled	Scaled	IR intensity	Raman active	Unscaled	Scaled	IR intensity	Raman active	Assignments
A	1488(ms)	-	1603	1485	6.7119	9.1792	1483	1485	8.0047	8.0505	νCC (80)
A	1446(ms)	-	1597	1440	25.2877	7.3726	1473	1442	27.0126	27.0126	νCC (82)
A	-	1440 (w)	1570	1438	1.8993	3.1032	1451	1438	2.5180	5.8053	CH_3 ipb (80)
A	1376 (w)	-	1551	1366	0.8973	9.2295	1423	1375	0.8919	22.5779	CH_3 ipb (81)
A	-	1365 (s)	1546	1354	1.117	7.2059	1420	1360	1.4731	19.4246	CH_3 ipb (78)
A	1338 (vs)	-	1544	1345	0.1368	5.2721	1419	1336	0.4509	10.9122	CH_3 sb (79)
A	1306 (s)	-	1433	1312	2.0251	8.8316	1363	1300	18.7650	1.6813	CH_3 sb (76)
A	-	1300 (s)	1425	1307	66.1678	3.7685	1338	1299	6.2135	23.5772	CH_3 sb (75)
A	1272 (s)	-	1367	1278	71.3789	4.6711	1296	1270	16.8657	1.5262	νCO (74)
A	-	1256 (vw)	1338	1261	60.6588	2.7134	1260	1255	48.7272	1.7297	bOH (72)
A	1226(ms)	1230 (w)	1280	1234	36.7928	2.7517	1215	1228	129.7939	3.7042	bCH (71)
A	1202(ms)	-	1263	1215	38.6501	6.2146	1176	1205	32.1744	6.3985	b CH (70)
A	-	1196 (w)	1164	1200	2.9144	0.1003	1062	1198	0.3946	0.1192	CH_3 opb (72)
A	1160(ms)	-	1161	1172	0.3697	0.4058	1061	1157	4.0698	1.6840	CH_3 opb (68)
A	-	1150 (vw)	1153	1159	0.1336	0.5953	1056	1145	2.5354	0.2580	CH_3 opb (71)
A	1031(ms)	-	1118	1035	8.8292	2.2987	1041	1034	18.8843	0.7846	Rtrigd (69)
A	1012 (w)	1010 (w)	1111	1018	12.6543	1.5019	1033	1011	1.2307	2.1304	Rsymd (68)
A	969 (w)	-	1082	975	16.3291	0.2363	1024	965	10.9027	0.4325	Rasymd (67)
A	-	958 (ms)	1038	963	0.9292	11.6543	972	954	6.6623	12.8851	CH_3 opr (66)
A	932 (ms)	-	1010	939	0.4895	0.3588	937	930	7.2656	0.0912	CH_3 opr (69)
A	-	920 (w)	1002	925	7.2172	0.6959	895	921	0.7823	0.5820	CH_3 opr (68)
A	-	880 (vw)	974	887	30.2844	0.2025	867	883	21.9720	0.2324	CH_3 ipr (69)
A	853 (vs)	-	828	850	11.0892	7.9539	772	851	11.9575	8.0693	CH_3 ipr (66)

(Contd.)

Table 4 — The observed FTIR, FT-Raman and calculated (unscaled and scaled) frequencies (cm^{-1}), IR intensity (km mol^{-1}), Raman Activity ($Å^4$ amu^{-1}), and probable assignments (characterized by TED) of 2,4,6-trimethylphenol using HF/6-31+G(d,p) and B3LYP/6-31+G(d,p) calculations (*Contd*.)

Species	Observed wave numbers (Cm^{-1})										
	FTIR	FT Raman	Unscaled	Scaled	IR intensity	Raman active	Unscaled	Scaled	IR intensity	Raman active	Assignments
A	762 (s)	765 (s)	811	778	6.2519	0.3464	725	764	3.2274	0.3194	CH_3 ipr (65)
A	723 (s)	-	635	718	2.8140	0.0583	583	720	5.7534	4.7181	b CC (65)
A	711 (ms)	-	627	715	6.4734	4.8127	581	710	2.0944	2.2541	b CC (64)
A	706 (ms)	-	608	710	0.0670	27.5733	575	705	0.3225	21.8820	b CC (66)
A	701 (w)	-	556	704	0.0005	0.2798	506	702	1.5654	0.6987	b CO (65)
A	682 (ms)	-	542	690	3.3078	1.8179	504	680	1.2418	0.6646	ω CH (61)
A	-	578 (s)	495	575	2.3854	6.5875	463	575	2.0786	6.2511	ω CH (62)
A	565 (w)	-	392	560	0.1399	1.5869	356	561	0.1790	1.1791	t Rtrigd (60)
A	-	520 (vw)	354	528	4.4151	0.0772	327	518	4.2889	0.0645	t Rsymd (61)
A	501 (w)	501 (w)	300	505	1.2175	0.4527	291	503	84.0559	0.8050	t R asymd (60)
A	493 (w)	-	289	490	0.7327	0.4738	279	492	1.1223	0.7033	ω CC (58)
A	482 (vw)	-	265	484	21.5225	1.1967	270	480	0.8721	0.7620	ω CC (59)
A	457 (vw)	460 (w)	203	455	81.1367	1.6465	227	458	12.0682	2.8984	ω CC (60)
A	426 (vw)	-	187	420	7.5536	0.3690	177	425	4.1993	0.0742	ω CO (61)
A	-	385 (ms)	168	370	6.2440	0.1587	152	383	0.3022	0.0478	ω OH (58)
A	-	350 (vw)	146	342	1.6362	0.3496	130	352	0.0088	0.2160	CH_3 twist (57)
A	-	277 (w)	131	271	1.6830	0.1357	121	274	0.0114	0.1234	CH_3 twist (56)
A	-	251 (w)	36	248	1.933	0.1738	42	252	0.2795	0.3889	CH_3 twist (57)

Abbreviations: w-weak, s-strong, ms-medium strong, vw-very weak, vs-very strong, R-ring, b-bending, v-stretching, symd-symmetric deformation, ω-out-of-plane bending, asymd-antisymmetric deformation, trigd-trigonal deformation, ss-symmetric stretching, ips-in-plane stretching, sb-symmetric bending, ipb-in-plane-bending, ipr-in-plane-rocking, ops-out-of-plane stretching, opb-out-of-plane bending, opr-out-of-planerocking, t-torsion.Table 5 – Thermodynamic properties of 3-methyl-4-nitrophenol and 2,4,6-trimethylphenol.

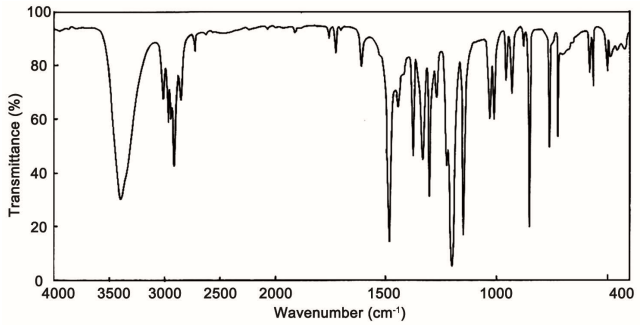

Fig. 2 — FTIR spectrum of 2,4,6-trimethylphenol.

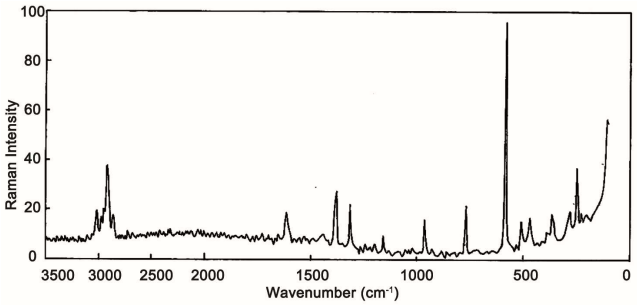

Fig. 3 — FT-Raman spectrum of 2,4,6-trimethylphenol.

deformation vibration in phenols lies in the region 290-320 cm^{-1} for free O-H and in the region 517-710 cm^{-1} for associated O-H[20]. In TMP, the FTIR band observed at 3396 cm^{-1} is assigned to O-H stretching vibration. The in-plane and out-of-plane bending vibrations of hydroxyl groups in FT-Raman have been identified at 1256, 385 cm^{-1} for TMP, respectively.

3.2.2 C-H Vibrations

Aromatic compounds commonly exhibit multiple weak bands in the region 3100-3000 cm^{-1} due to aromatic C-H stretching vibrations[21]. The bands due to C-H in-plane ring bending vibrations, interact somewhat with C-C stretching vibrations, are observed as a number of sharp bands in the region 1300 -1000 cm^{-1}. The C-H out-of-plane bending vibrations are strongly coupled vibrations and occur in

the region 900 - 667 cm^{-1}. Hence, the Raman bands found at 3380, 3100 cm^{-1} in TMP have been assigned to C-H stretching vibrations, respectively. The in-plane and out-of-plane bending vibrations of C-H group have also been identified for TMP and they were presented in Table 4.

3.2.3 CH_3 Vibrations

The title compound under consideration possesses a CH_3 group in the side-substituted chain. For the assignments of CH_3 group frequencies, one can expect that nine fundamental vibrations can be associated with each CH_3 group, namely the symmetrical stretching in CH_3 (CH_3 symmetric stretch) and asymmetrical stretching (CH_3 asymmetric stretch) in-plane stretching modes (i.e., in-plane hydrogen stretching mode); the symmetrical (CH_3 symmetric deform) and asymmetrical (CH_3 asymmetric deform) deformation modes; the in-plane rocking (CH_3 ipr), out-of-plane rocking (CH_3 opr) and twisting (tCH_3) modes. Methyl groups are generally referred as electron-donating substituent in the aromatic ring system.

For the assignments of CH_3 group frequencies, nine fundamental vibrations can be associated with each CH_3 group. Three stretching, three bending, two rocking modes and a single torsional mode describe the motion of the methyl group[22]. Hence in the present investigation the FTIR bands observed at 3013 cm^{-1} for TMP, respectively and the FT-Raman bands observed at 3019, 2980 cm^{-1} for TMP have been designated to CH_3 symmetric stretching vibrations. The FTIR bands found at 2973, 2944, 2917 cm^{-1} for TMP and the Raman bands found at 2918 cm^{-1} for TMP are assigned to CH_3 in-plane stretching vibrations. The FTIR and Raman bands observed at 1320 cm^{-1} in IR and 1300 cm^{-1} in Raman for TMP have been designated to CH_3 symmetric bending vibrations. The CH_3 in-plane bending vibrations observed at 1376 cm^{-1} in FTIR and in Raman 1440, 1365 cm^{-1} for TMP. The fundamental vibrations arising from symmetric, asymmetric in-plane and out-of–plane deformations, rocking and twisting modes of CH_3 group of TMP were observed in their respective characteristic regions and they were listed in Table 4.

3.2.4 C-O vibrations

The interaction of carbonyl group with other groups present in the system does not produce such a drastic and characteristics changes in the frequency of C-O stretch as did by the interaction of N-H stretch. In the present study, the Raman band observed at 1203 cm^{-1} in TMP has been assigned to C-O stretching vibrations. The in-plane and out-of-plane bending vibrations of C-O group are also found well within the characteristic region[23].

3.2.5 C-C Vibrations

The bands between 1400 and 1650 cm^{-1}, in benzene derivatives are due to C-C stretching vibrations[24]. Therefore, the C-C stretching vibrations of TMP are found at 1740, 1728, 1612, 1488 and 1446 cm^{-1} in the FTIR spectrum and at 1720, 1640, 1604, 1495 cm^{-1} in the FT-Raman spectrum. The C-C in-plane and out-of-plane bending vibrations of the title compounds were well identified in the recorded spectra within their characteristic region.

3.3 Vibrational contribution to NLO activity and first hyperpolarizability

The potential application of the title compound in the field of nonlinear optics demands the investigation of its structural and bonding features contributing to the hyperpolarizability enhancement, by analyzing the vibrational modes using IR and Raman spectroscopy. The first hyperpolarizability (β) of this novel molecular system is calculated using the *ab initio* quantum mechanical method, quantum mechanical method, based on the finite-field approach. In the presence of an applied electric field, the energy of a system is a function of the electric field. The first hyperpolarizablity is a third-rank tensor that can be described by a 3×3×3 matrix. The 27 components of the 3D matrix can be reduced to 10 components due to the Kleinman symmetry[25].

The components of β are defined as the coefficients in the Taylor series expansion of the energy in the external electric field. When the electric field is weak and homogeneous, this expansion becomes:

$$E = E_0 - \sum_{i} \mu_i F^i \frac{1}{2} \sum_{ij} \alpha_{ij} F^i F^j \frac{1}{6} \sum_{ijk} \beta_{ijk} F^i F^j F^k \frac{1}{24} \sum_{ijkl} \nu_{ijkl} F^i F^j F^k F^l + \cdots$$

where E_0 is the energy of the unperturbed molecule; F^i is the field at the origin; and μ_i, α_{ij}, β_{ijk} and ν_{ijkl} are the components of dipole moment, polarizability, the first hyper polarizabilities and second hyperpolarizibilities, respectively. The calculated total dipole moment (μ) of the compound TMP is 1.4543 Debye. The calculated mean first hyperpolarizibility (β) of the compound TMP is 1.919×10^{-30} esu, which is comparable with the reported values of similar derivatives[26]. The large value of hyperpolarizibility (β) which is a measure of the non-linear optical activity of the molecular system, is

Table 5 — Thermodynamic properties of 3-methyl-4-nitrophenol and 2,4,6-trimethylphenol.

Parameters	MNP		TMP	
	HF/6 -31+G(d,p)	B3LYP/6 -31+G(d,p)	HF/6 -31+G(d,p)	B3LYP/6 -31+G(d,p)
Self consistent field energy (a.u)	-548.0975	-551.3229	-422.7019	-425.4559
Zero point vibrational energy (kcal/Mol)	91.24370	84.66606	125.1619	117.2883
Rotational constants, *A* (GHz)	2.26938	2.22252	1.7575	1.7376
B (GHz)	0.81789	0.80070	1.2688	1.2518
C (GHz)	0.60452	0.59140	0.7469	0.7376
Entropy (Cal/Mol-Kelvin)	95.036	98.195	99.135	100.731
Specific heat capacity (C_v) (Cal/Mol-Kelvin)	33.652	36.206	37.645	40.051
Translational and rotational energy (kCal/Mol-Kelvin)	0.889	0.889	0.889	0.889
Vibrational energy (kCal/Mol-Kelvin)	95.076	88.869	129.866	122.296
Dipole moment (Debye) (μ_{total})	5.4494	5.5151	1.4543	1.4139

associated with the intramolecular charge transfer, resulting from the electron cloud movement through π conjugated frame work from an electron donor to electron acceptor groups. The physical properties of these conjugated molecules are governed by the high gaps. So, we conclude that the title compounds are an attractive object for future studies of nonlinear optical properties.

3.4 Other molecular properties

In addition to the vibrational assignments, several thermodynamic parameters are also calculated on the basis of vibrational analysis at HF/6-31+G (d,p) and B3LYP/6-31+G (d,p). The calculated thermodynamic properties are presented in the Table 5. The self consistent field (SCF) energy, zero point vibrational energies (ZPVE), rotational constants, dipole moment and entropy S_{Vib} (*T*) are calculated to the extent of accuracy and the variations in the ZPVEs seem to be insignificant. The total energies and change in total entropy of 2,4,6-trimethylphenol (TMP) at room temperature are only marginal.

The highest occupied molecular orbital (HOMO) and the lowest unoccupied molecular orbital (LUMO) are named as frontier molecular orbital's (FMOs). The FMOs play an important role in the electrical and optical properties, as well as in UV–Vis spectra and chemical reactions. The transitions from the HOMO to the LUMO are mainly derived from the electronic transitions of $\pi \rightarrow \pi^*$. This is confirmed by analyzing the UV–Vis spectra. The peak obtained in UV–Vis spectra results from $\pi \rightarrow \pi^*$ transition of aromatic ring system.

The molecular electrostatic potential (MEP) has been used extensively for the analysis of molecular interactions, including chemical reactions, hydrogen bonding, salvation processes and bio molecular recognition interactions. It provides a visual method to understand the relative polarity of the molecule. An electron density is surface mapped with electrostatic potential surface depicts the size, shape, charge density and site of chemical reactivity of the molecules.

4 Conclusions

The SQM force field method based on DFT calculations at the HF/6-31+G(d,p) and B3LYP/6-31+G (d,p) levels has been carried out to analyze the vibrational frequencies of 2,4,6-trimethylphenol. The close agreement established between the experimental and scaled frequencies obtained by B3LYP using the large basis set (6-31+G (d,p)) calculation is proved to be more reliable and accurate than the calculations of semi-empirical methods or lower basis sets. This accuracy is desirable for resolving disputes in vibrational assignments and provides valuable insight for understanding the observed spectral features. In addition, thermodynamic functions of TMP were also presented. The first hyperpolarizability (β) of these novel molecular systems was calculated.

References

1 Varasanyi G, *Assignments of vibrational spectra of seven hundred benzene derivatives*, (Adam Hilger), 1974.
2 Evans J C, *Spectrochim Acta A*, 16 (1960) 1382.
3 Bist H D, Brand J C D & Williams D R, *J Mol Spectrosc*, 24 (1967) 402.
4 Sundaraganesan N, Illakiamani S, Saleem H, Wojiciechowski P M & Minchalska D, *Spectrochim Acta A*, 61 (2005) 2995.
5 Zhengyu Z & Dongmet D, *J Mol Struct Theochem,* 505 (2000) 247.
6 Stephens P J, Devlin F J, Chavalowski C F & Frisch M J, *J Phys Chem*, 98 (1994) 11623.

7 Devlin F J, Finley J W, Stephens P J & Frish M J, *J Phys Chem*, 99 (1995) 16883.

8 Lee S Y & Boo B H, *Bull Kor Chem Soc*, 17 (1996) 760.

9 Nagabalasubramanian P B, Periandy S & Mohan S, *Spectrochim Acta*, A77 (2010) 150.

10 Sundaraganesan N & Dominic J B, *Spectrochim Acta*, 68 (2007) 771.

11 Frisch M J, Trucks G W, Schlegal H B, Scuseria G E, Robb M A, Cheesman J R, Zakrzewski V G, Montgomerg J A, Stratman J, Burant J C, Dapprich S, Millam J M, Daniels A D, Kudin K N, Strain M C, Farkas O, Tomasi J, Barone V, Cossi M, Cammi R, Mennucci B, Pomelli C, Adamo C, Clifford S, Ochterski J, Petersson G A, Ayala P Y, Cui Q, Morokuma K, Rega N, Salvador P, Dannenberg J J, Malich D K, Rabuck A D, Raghavachari K, Foresman J B, Cioslowski J, Ortiz J V, Baboul A G, Stetanov B B, Liu G, Liashenko A, Piskorz P, Komaromi I, Gomperts R, Martin R L, Fox D J, Keith T, Al-Laham M A, Peng C Y, Nanayakkara A, Challacombe M, Gill P M W, Johnson B, Chen W, Wong M W, Andres J L, Gonzalez C, Head-Gordon M, Replogle E S & Pople J A, *GAUSSIAN 09, Revision A 114*, (Gaussian Inc: Pittsburgh PA), 2009.

12 Schlegal H B, *J Comput Chem*, 3 (1982) 214.

13 Hohenberg P & W Kohu, *Phys Rev*, 136 (1964) 864.

14 Becke A D, *J Chem Phys*, 98 (1993) 5648.

15 Lee C, Yang W & Parr R G, *Phys Rev*, 37 (1988) 785.

16 Frisch A, Nielson A B & Holder A J, *Gauss view users manual,* (Gaussian Inc: Pittsburgh PA), 2004.

17 Keresztury G, *Raman spectroscopy theory*, in: Chalmers J M & Griffiths P R (Edn), *Handbook of vibrational spectroscopy*, (John Wiley & Sons Ltd), 1 (2002) 71.

18 Keresztury G, Holly S, Varga J, Besenyei G, Wang A Y & Durig J R, *Spectrochim Acta Part A*, 49 (1993) 2007.

19 Sathyanarayana D N, *Vibrational spectroscopy - theory and applications*, 2nd Edn, (New Age International (P) Limited Publishers: New Delhi), 2004.

20 Arivazhagan M & Krishnakumar V, *Indian J Pure Appl Phys*, 43 (2005) 573.

21 Sajan D, Binoy J, Hubert Joe I, Jayakumar V S & Zaleski J, *Raman Spectrosc*, 36 (2005) 221.

22 Socrates G, *Infrared and Raman characteristic group frequencies - tables and charts*, 3rd Edn, (Wiley: Chichester), 2001.

23 Chithambarathanu T, Umayourbagan V & Krishnakumar V, *Indian J Pure Appl Phys*, 40 (2002) 72.

24 Goel R K & Sharma S D, *Indian J Pure Appl Phys*, 19 (1981) 472.

25 Kleinman D A, *Phys Rev*, 126 (1962) 1977.

26 Anto P L, Ruby J A, Hema T V, Yohannan P C & Daizy P, *J Raman Spectrosc*, 41 (2010) 113.